

# Accurate renormalization group analyses in neutrino sector

Yuya Yamaguchi (Hokkaido Univ., Japan)

Collaborators : N.Haba, R.Takahashi (Shimane Univ.),  
and K.Kaneta (Tokyo Univ., ICRR)

[arXiv:1402.4126](https://arxiv.org/abs/1402.4126)

[Nucl. Phys. B 885 \(2014\) 180-195](#)

# Introduction

- Light neutrinos are very different from other fermions

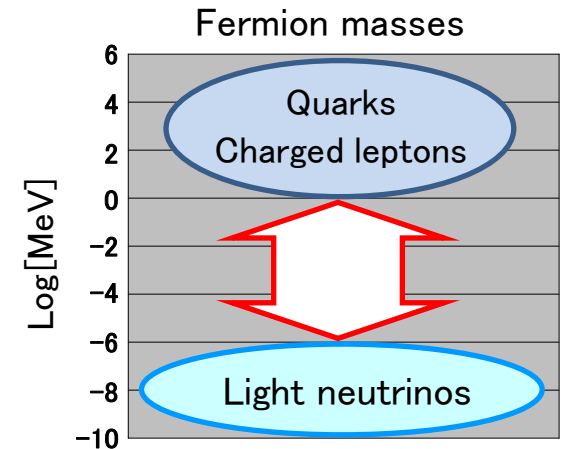
- Smallness of masses



- Structure of mixing angles

CKM matrix:  $\theta_{12} = 13^\circ$ ,  $\theta_{23} = 2.4^\circ$ ,  $\theta_{13} = 0.2^\circ$

PMNS matrix:  $\theta_{12} \simeq 33^\circ$ ,  $\theta_{23} \simeq 41^\circ$ ,  $\theta_{13} \simeq 8.8^\circ$

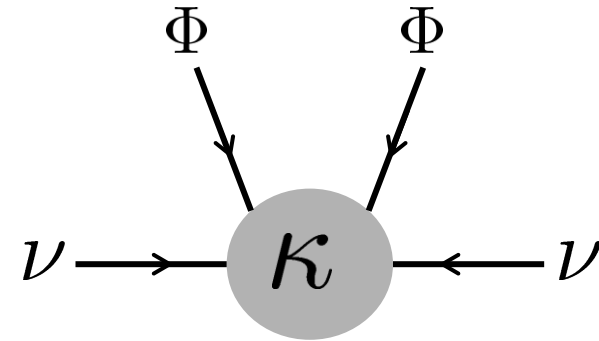


- The behavior may suggest high energy physics beyond the SM
  - Ex.) Seesaw mechanism, flavor symmetry, etc.
- In order to know the high energy behavior accurately, we consider decoupling effects of top quark and Higgs boson on the RGEs of light neutrino mass matrix

# Light neutrino mass matrix

- Lepton mass terms

$$\mathcal{L} = -Y_E \bar{L} \Phi E_R - \frac{\kappa}{2} (\bar{L}^C \Phi)(L \Phi)$$



$\kappa$  : coefficient of an effective dim. 5 operator

- Light neutrino mass matrix

$$M_\nu = \kappa v^2$$

$v$  is a relevant Higgs vacuum expectation value:

$$v = \begin{cases} 174 \text{ GeV in the SM} \\ 174 \times \sin \beta \text{ GeV in the MSSM} \end{cases}$$

# Renormalization group equation for $\kappa$

- RGE for  $\kappa$  at one-loop level

$$16\pi^2 \frac{d\kappa}{dt} = C_E (Y_E^\dagger Y_E)^T \kappa + C_E \kappa (Y_E^\dagger Y_E) + \bar{\alpha} \kappa$$

$$\begin{cases} \bar{\alpha}_{\text{SM}} = 2 \text{Tr} [3Y_U^\dagger Y_U + 3Y_D^\dagger Y_D + Y_E^\dagger Y_E] - 3g_2^2 + \lambda \\ \bar{\alpha}_{\text{MSSM}} = 6 \text{Tr} [Y_U^\dagger Y_U] - \frac{6}{5}g_1^2 - 6g_2^2 \end{cases}$$

where  $t = \ln \mu$ , and  $C_E = -3/2$  (1) in the SM (MSSM)

S.Antusch, M.Drees, J.Kersten, M.Lindner, and M.Ratz (2001)

- Solving this equation,  $M_\nu (= \kappa v^2)$  is written by

$$M_\nu(\Lambda) = R \left( I M_\nu(\Lambda_{\text{EW}}) I \right) \quad \text{J.R.Ellis and S.Lola (1990)}$$

High energy
Low energy

$$I^{-1} \equiv \text{Diag}\{\sqrt{I_e}, \sqrt{I_\mu}, \sqrt{I_\tau}\}, \quad I_\alpha \equiv \exp \left[ -\frac{C_E}{8\pi^2} \int_{t_{\text{EW}}}^{t_\Lambda} dt y_\alpha^2 \right] \quad (\alpha = e, \mu, \tau)$$

# Neutrino mass matrix with $r$ and $\epsilon$

- Then, neutrino mass matrix is written by

$$M_\nu(\Lambda) = \frac{R}{I_e} \begin{pmatrix} (M_\nu(\Lambda_{EW}))_{ee} & (M_\nu(\Lambda_{EW}))_{e\mu} \sqrt{\frac{I_e}{I_\mu}} & (M_\nu(\Lambda_{EW}))_{e\tau} \sqrt{\frac{I_e}{I_\tau}} \\ (M_\nu(\Lambda_{EW}))_{e\mu} \sqrt{\frac{I_e}{I_\mu}} & (M_\nu(\Lambda_{EW}))_{\mu\mu} \frac{I_e}{I_\mu} & (M_\nu(\Lambda_{EW}))_{\mu\tau} \sqrt{\frac{I_e}{I_\mu} \frac{I_e}{I_\tau}} \\ (M_\nu(\Lambda_{EW}))_{e\tau} \sqrt{\frac{I_e}{I_\tau}} & (M_\nu(\Lambda_{EW}))_{\mu\tau} \sqrt{\frac{I_e}{I_\mu} \frac{I_e}{I_\tau}} & (M_\nu(\Lambda_{EW}))_{\tau\tau} \frac{I_e}{I_\tau} \end{pmatrix}$$

- We define  $r \equiv R/I_e$ ,  $\epsilon_\tau \equiv \sqrt{I_e/I_\tau} - 1$  and  $\epsilon_\mu \equiv \sqrt{I_e/I_\mu} - 1$
- Since  $\epsilon_\mu$  is numerically almost equal to 0, **we can neglect  $\epsilon_\mu$**

- Finally, neutrino mass matrix is approximately written by

$$M_\nu(\Lambda) \simeq r \begin{pmatrix} (M_\nu(\Lambda_{EW}))_{ee} & (M_\nu(\Lambda_{EW}))_{e\mu} & (M_\nu(\Lambda_{EW}))_{e\tau} (1 + \epsilon) \\ (M_\nu(\Lambda_{EW}))_{e\mu} & (M_\nu(\Lambda_{EW}))_{\mu\mu} & (M_\nu(\Lambda_{EW}))_{\mu\tau} (1 + \epsilon) \\ (M_\nu(\Lambda_{EW}))_{e\tau} (1 + \epsilon) & (M_\nu(\Lambda_{EW}))_{\mu\tau} (1 + \epsilon) & (M_\nu(\Lambda_{EW}))_{\tau\tau} (1 + \epsilon)^2 \end{pmatrix}$$

where we redefine  $\epsilon \equiv \epsilon_\tau$

N.Haba and R.Takahashi (2013)

# Neutrino mass matrix with $r$ and $\epsilon$

- $r$  and  $\epsilon$  are calculated by

$$r(\Lambda) = \frac{(M_\nu(\Lambda))_{ee}}{(M_\nu(\Lambda_{EW}))_{ee}}, \quad \epsilon(\Lambda) = \exp \left[ \frac{1}{2} \frac{C_E}{8\pi^2} \int_{t_{EW}}^{t_\Lambda} dt (y_\tau^2 - y_e^2) \right] - 1$$

- $M_\nu(\Lambda_{EW})$  is given by PMNS matrix (assuming mass eigenvalues):

$$(M_\nu)_{\alpha\beta} = \sum_i U_{\alpha i}^* U_{\beta i} m_i$$

$$U = \begin{pmatrix} c_{12}c_{13} & s_{12}c_{13} & s_{13}e^{-i\delta} \\ -s_{12}c_{23} - c_{12}s_{23}s_{13}e^{i\delta} & c_{12}c_{23} - s_{12}s_{23}s_{13}e^{i\delta} & s_{23}c_{13} \\ s_{12}s_{23} - c_{12}c_{23}s_{13}e^{i\delta} & -c_{12}s_{23} - s_{12}c_{23}s_{13}e^{i\delta} & c_{23}c_{13} \end{pmatrix} \begin{pmatrix} e^{-i\frac{\phi_1}{2}} & 0 & 0 \\ 0 & e^{-i\frac{\phi_2}{2}} & 0 \\ 0 & 0 & 1 \end{pmatrix}$$

- Mass squared differences and mixing angles in the EW scale:

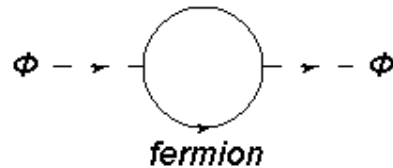
| $\Delta m_{21}^2$                 | $\Delta m_{31}^2$                      | $\sin^2 \theta_{12}$ | $\sin^2 \theta_{23}$ | $\sin^2 \theta_{13}$ |
|-----------------------------------|--|----------------------|----------------------|----------------------|
| $7.54 \times 10^{-5} \text{eV}^2$ | $2.48 \times 10^{-3} \text{eV}^2$ (NH) | 0.308                | 0.425 (NH)           | 0.0234 (NH)          |
|                                   | $2.44 \times 10^{-3} \text{eV}^2$ (IH) |                      | 0.437 (IH)           | 0.0239 (IH)          |

– We assume  $\Lambda_{EW} = M_Z$

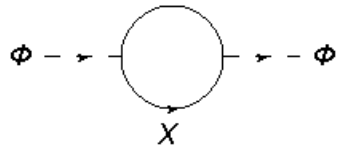
F.Capozzi, et al., arXiv:1312.2878.

# Decoupling theorem

- The RGEs in the previous slide are effective for  $m_t^{\text{pole}} \leq \mu < \underline{M_a}$ 
    - For  $\mu < m_t^{\text{pole}}$  top quark is decoupled
    - For  $\mu < m_h$  Higgs boson is also decoupled
    - :
- cutoff scale  
Effective theory is valid  
in this region
- One of the quantum effects by fermions are shown by



- Decoupling theorem says that, for  $\mu < m_x$  (x is some fermion)
- $\phi \rightarrow \phi$  already does not contribute to quantum effects  
(neglecting threshold corrections)  
T.Appelquist and J.Carazzone (1975)



# RGEs in the SM for $\mu \geq m_t^{\text{pole}}$

$$16\pi^2\beta_\kappa = -\frac{3}{2}(Y_E^\dagger Y_E)^T \kappa - \frac{3}{2}\kappa (Y_E^\dagger Y_E) + 2\text{Tr} \left[ 3Y_U^\dagger Y_U + 3Y_D^\dagger Y_D + Y_E^\dagger Y_E \right] \kappa - 3g_2^2 \kappa + \lambda \kappa,$$

$$16\pi^2\beta_{Y_U} = Y_U \left\{ \frac{3}{2}Y_U^\dagger Y_U - \frac{3}{2}Y_D^\dagger Y_D + \text{Tr} \left[ 3Y_U^\dagger Y_U + 3Y_D^\dagger Y_D + Y_E^\dagger Y_E \right] - \frac{17}{20}g_1^2 - \frac{9}{4}g_2^2 - 8g_3^2 \right\},$$

$$16\pi^2\beta_{Y_D} = Y_D \left\{ \frac{3}{2}Y_D^\dagger Y_D - \frac{3}{2}Y_U^\dagger Y_U + \text{Tr} \left[ 3Y_U^\dagger Y_U + 3Y_D^\dagger Y_D + Y_E^\dagger Y_E \right] - \frac{1}{4}g_1^2 - \frac{9}{4}g_2^2 - 8g_3^2 \right\},$$

$$16\pi^2\beta_{Y_E} = Y_E \left\{ \frac{3}{2}Y_E^\dagger Y_E + \text{Tr} \left[ 3Y_U^\dagger Y_U + 3Y_D^\dagger Y_D + Y_E^\dagger Y_E \right] - \frac{9}{4}g_1^2 - \frac{9}{4}g_2^2 \right\},$$

$$16\pi^2\beta_\lambda = 6\lambda^2 - \left( \frac{9}{5}g_1^2 + 9g_2^2 \right) \lambda + \frac{9}{2} \left( \frac{3}{25}g_1^4 + \frac{2}{5}g_1^2 g_2^2 + g_2^4 \right) + 4\text{Tr} \left[ 3Y_U^\dagger Y_U + 3Y_D^\dagger Y_D + Y_E^\dagger Y_E \right] \lambda - 8\text{Tr} \left[ 3Y_U^\dagger Y_U Y_U^\dagger Y_U + 3Y_D^\dagger Y_D Y_D^\dagger Y_D + Y_E^\dagger Y_E Y_E^\dagger Y_E \right].$$



# RGEs in the SM for $m_h \leq \mu < m_t^{\text{pole}}$

Diagrams with internal line of top quark do not contribute.

$$16\pi^2\beta_\kappa = -\frac{3}{2}(Y_E^\dagger Y_E)^T \kappa - \frac{3}{2}\kappa (Y_E^\dagger Y_E) + 2 \left( \text{Tr} \left[ 3Y_U^\dagger Y_U + 3Y_D^\dagger Y_D + Y_E^\dagger Y_E \right] - 3y_t^2 \right) \kappa - 3g_2^2 \kappa + \lambda\kappa,$$

$$16\pi^2\beta_{Y_{U \in \{y_u, y_c\}}} = Y_U \left\{ \frac{3}{2}Y_U^\dagger Y_U - \frac{3}{2}Y_D^\dagger Y_D + \left( \text{Tr} \left[ 3Y_U^\dagger Y_U + 3Y_D^\dagger Y_D + Y_E^\dagger Y_E \right] - 3y_t^2 \right) - \frac{17}{20}g_1^2 - \frac{9}{4}g_2^2 - 8g_3^2 \right\},$$

$$16\pi^2\beta_{y_b} = y_b \left\{ \frac{3}{2}y_b^2 + \left( \text{Tr} \left[ 3Y_U^\dagger Y_U + 3Y_D^\dagger Y_D + Y_E^\dagger Y_E \right] - 3y_t^2 \right) - \frac{1}{4}g_1^2 - \frac{9}{4}g_2^2 - 8g_3^2 \right\},$$

$$16\pi^2\beta_{Y_{D \in \{y_d, y_s\}}} = Y_D \left\{ \frac{3}{2}Y_D^\dagger Y_D - \frac{3}{2}Y_U^\dagger Y_U + \left( \text{Tr} \left[ 3Y_U^\dagger Y_U + 3Y_D^\dagger Y_D + Y_E^\dagger Y_E \right] - 3y_t^2 \right) - \frac{1}{4}g_1^2 - \frac{9}{4}g_2^2 - 8g_3^2 \right\},$$

$$16\pi^2\beta_{Y_E} = Y_E \left\{ \frac{3}{2}Y_E^\dagger Y_E + \left( \text{Tr} \left[ 3Y_U^\dagger Y_U + 3Y_D^\dagger Y_D + Y_E^\dagger Y_E \right] - 3y_t^2 \right) - \frac{9}{4}g_1^2 - \frac{9}{4}g_2^2 \right\},$$

$$16\pi^2\beta_\lambda = 6\lambda^2 - \left( \frac{9}{5}g_1^2 + 9g_2^2 \right) \lambda + \frac{9}{2} \left( \frac{3}{25}g_1^4 + \frac{2}{5}g_1^2 g_2^2 + g_2^4 \right) + 4 \left( \text{Tr} \left[ 3Y_U^\dagger Y_U + 3Y_D^\dagger Y_D + Y_E^\dagger Y_E \right] - 3y_t^2 \right) \lambda - 8 \left( \text{Tr} \left[ 3Y_U^\dagger Y_U Y_U^\dagger Y_U + 3Y_D^\dagger Y_D Y_D^\dagger Y_D + Y_E^\dagger Y_E Y_E^\dagger Y_E \right] - 3y_t^4 \right).$$

# RGEs in the SM for $M_Z \leq \mu < m_h$

Diagrams with internal line of Higgs boson also do not contribute.

$$16\pi^2 \beta_\kappa = -3g_2^2 \kappa,$$

$$16\pi^2 \beta_{y_t} = 0,$$

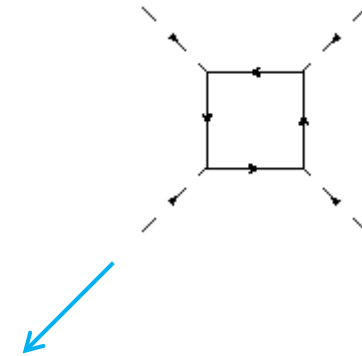
$$16\pi^2 \beta_{Y_{U \in \{y_u, y_c\}}} = Y_U \left( -\frac{2}{3}g_1^2 - 8g_3^2 \right),$$

$$16\pi^2 \beta_{Y_D} = Y_D \left( \frac{1}{5}g_1^2 - 8g_3^2 \right),$$

$$16\pi^2 \beta_{Y_E} = Y_E \left( -\frac{9}{5}g_1^2 \right),$$

$$16\pi^2 \beta_\lambda = -8 \left( \text{Tr} \left[ 3Y_U^\dagger Y_U Y_U^\dagger Y_U + 3Y_D^\dagger Y_D Y_D^\dagger Y_D + Y_E^\dagger Y_E Y_E^\dagger Y_E \right] - 3y_t^4 \right).$$

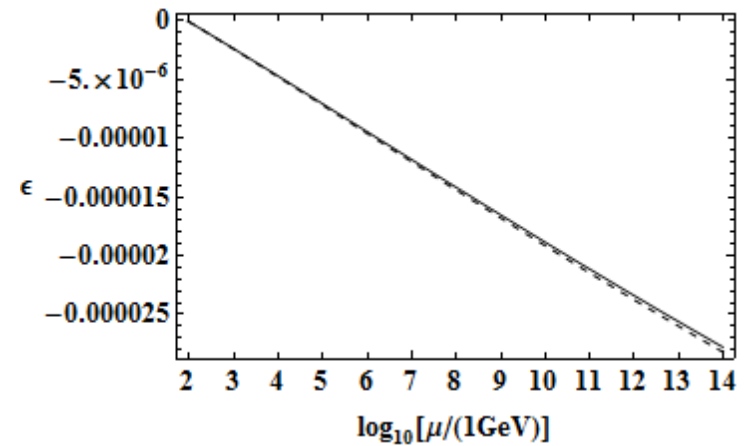
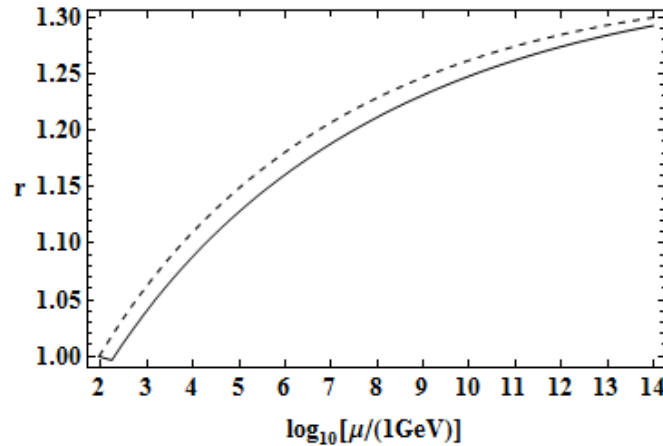
Fermion box diagram



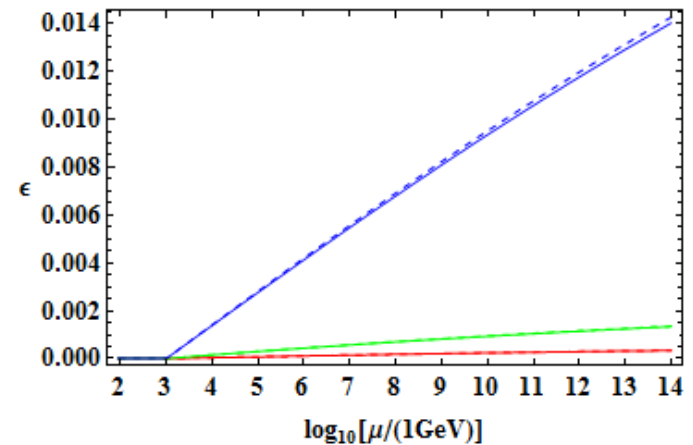
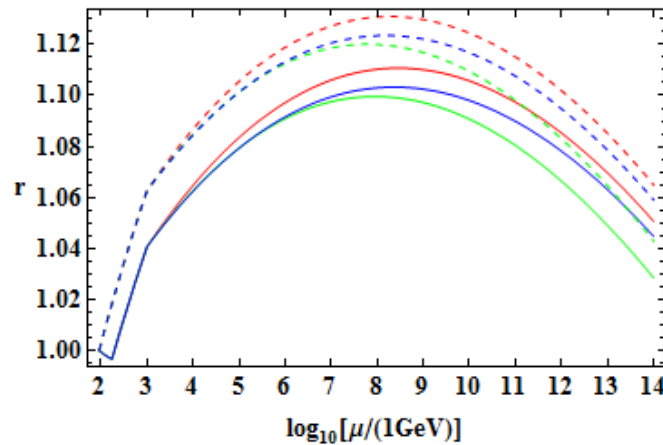
# Numerical results

# Runnings of $r$ and $\epsilon$

SM



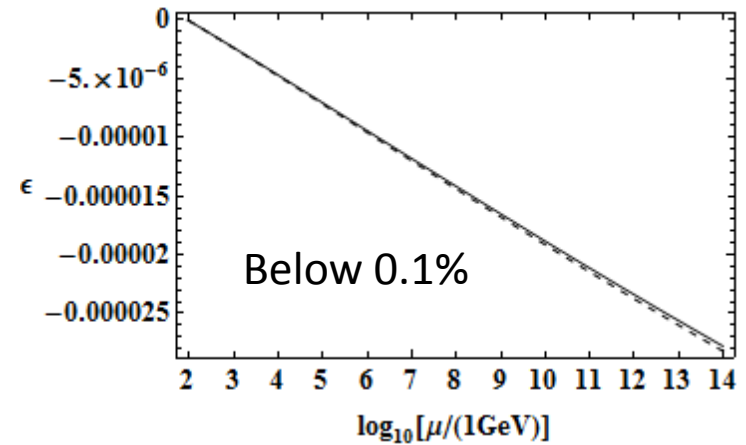
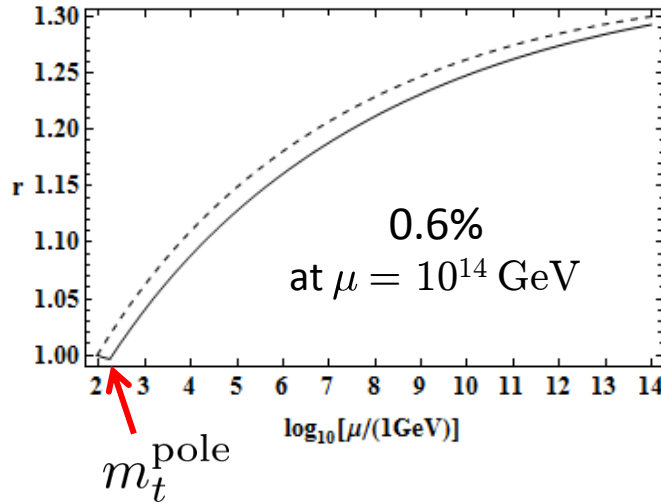
MSSM  
(SUSY = 1TeV)



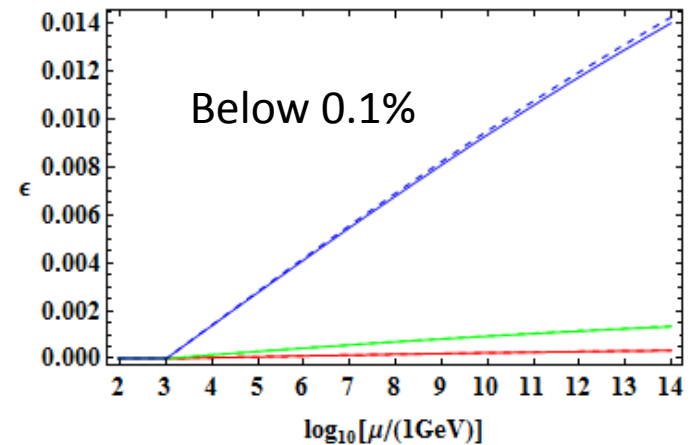
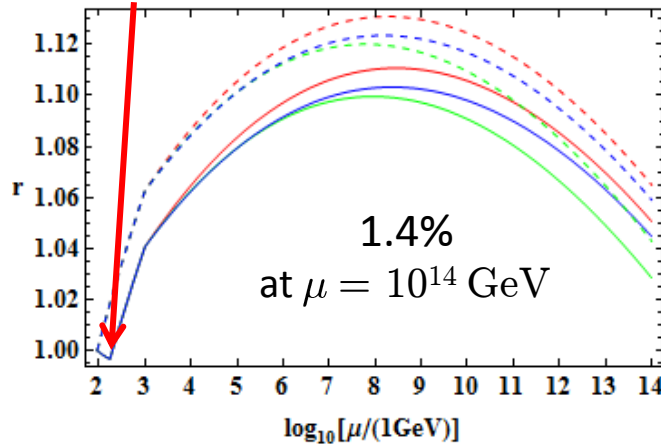
- Solid line: Including the decoupling effects
- Dashed line: Not including the decoupling effects
- Red, Green, and Blue lines:  $\tan\beta = 5, 10, \text{ and } 30$

# Runnings of $r$ and $\epsilon$

SM



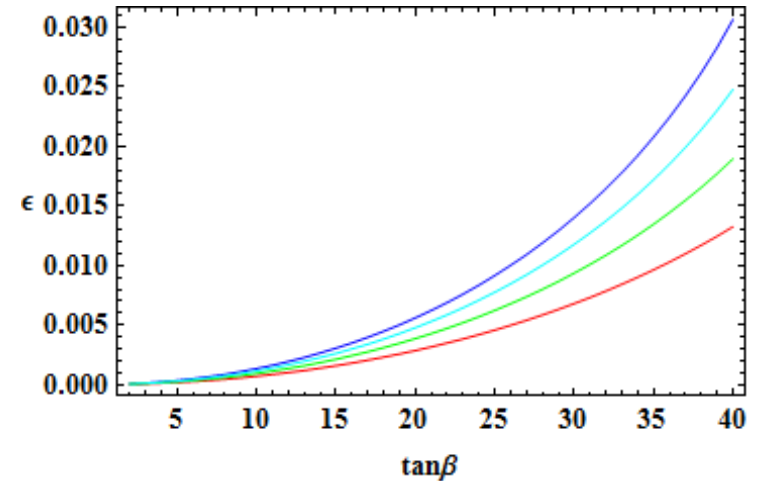
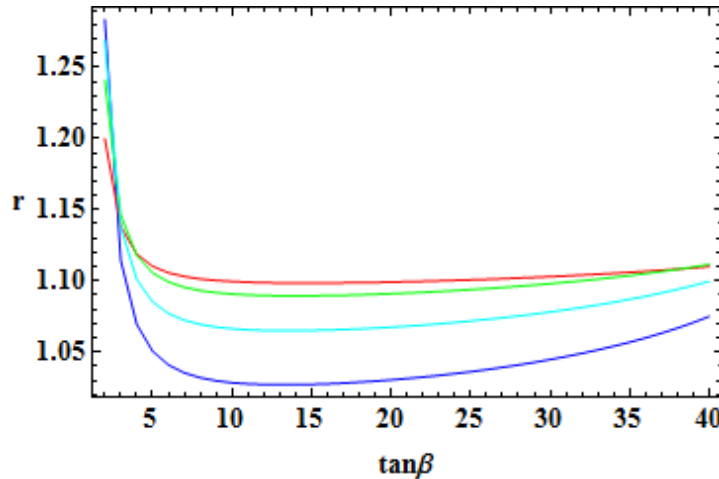
MSSM  
(SUSY = 1TeV)



- The differences between including the decoupling effects or not are not negligible for  $r$
- The main differences are occurred by top quark decoupling

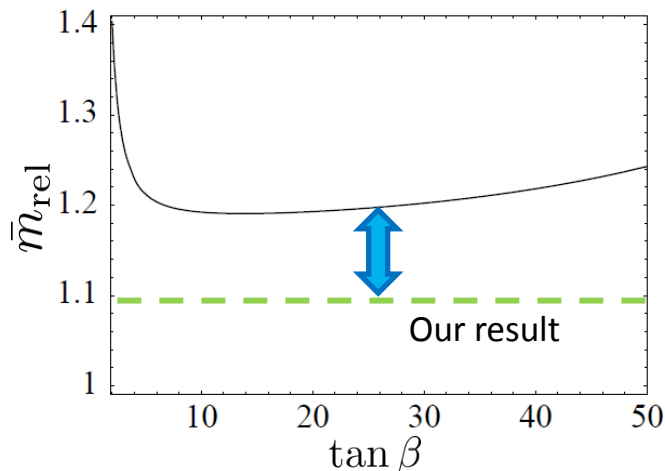
# $\tan\beta$ dependence of $r$ and $\epsilon$

MSSM  
(SUSY = 1TeV)



■ These figures are results including the decoupling effects

➤ Red, Green, Cyan and Blue lines:  $\mu = 10^8, 10^{10}, 10^{12},$  and  $10^{14}$  GeV



【Comparison with previous work】

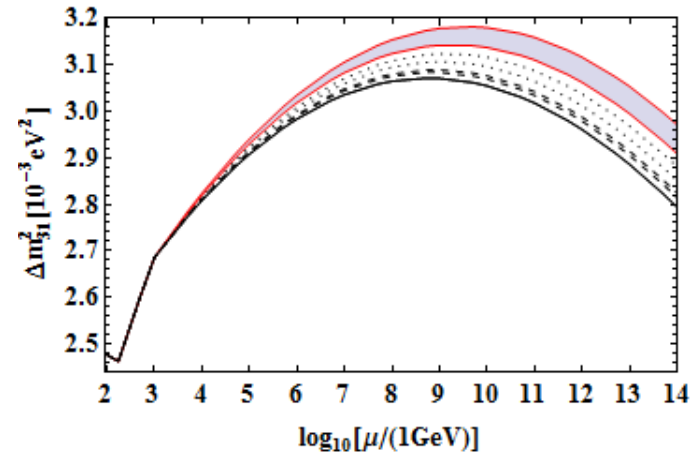
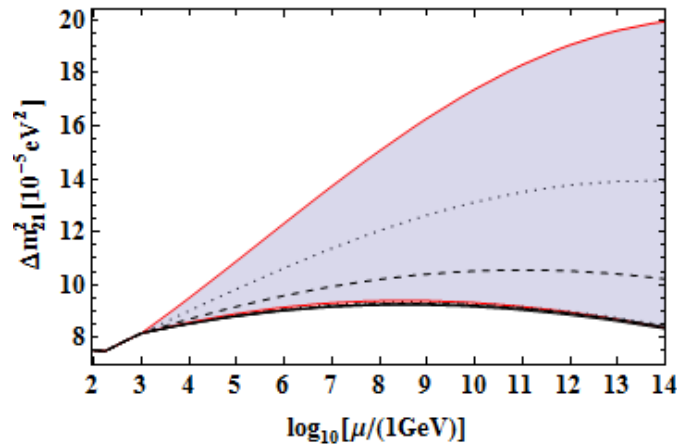
$$\bar{m} = \sqrt{m_1^2 + m_2^2 + m_3^2}, \quad \bar{m}_{\text{rel}} \equiv \frac{\bar{m}(10^{10} \text{ GeV})}{\bar{m}(M_Z)}$$

$\bar{m}_{\text{rel}}$  corresponds to the green line (upper left fig.)

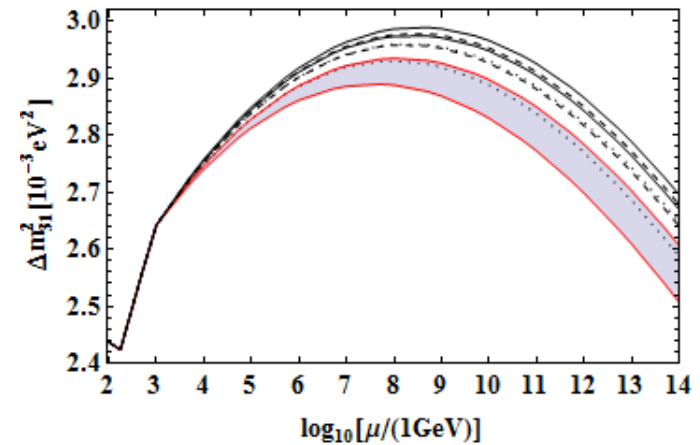
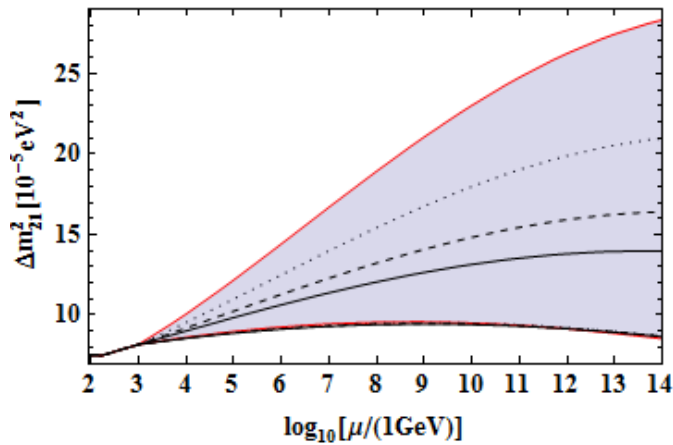
This value is important for leptogenesis.  
The difference between our result and previous work is not negligible.

# Runnings of mass squared differences

NH  
(SUSY = 1TeV,  
 $\tan\beta = 30$ )

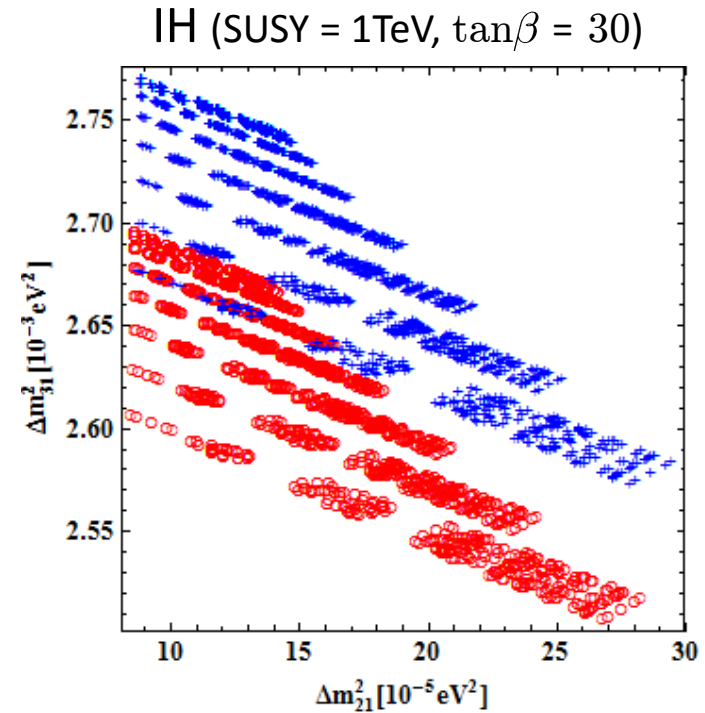
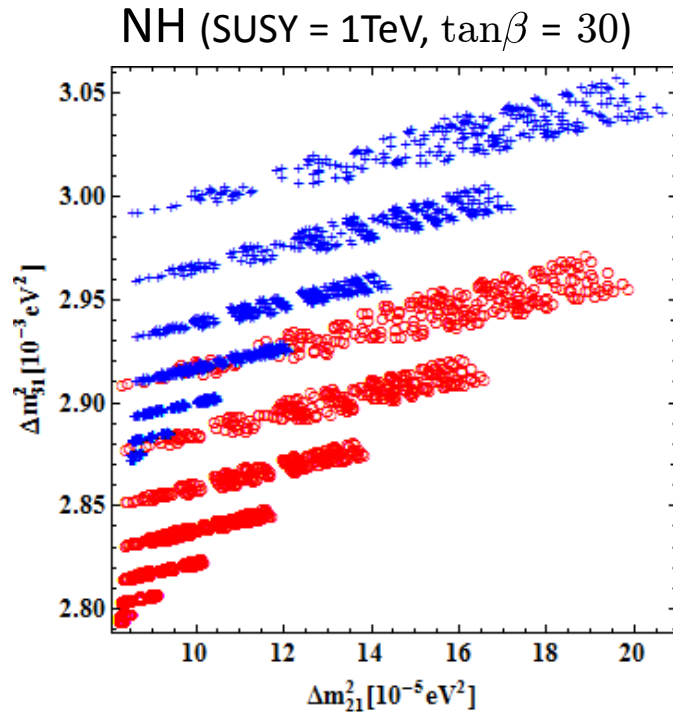


IH  
(SUSY = 1TeV,  
 $\tan\beta = 30$ )



- These figures are results including the decoupling effects
- Solid, dashed, dotted, and red-solid lines:  $m_{1(\text{or } 3)} = 0, 0.03, 0.05, \text{ and } 0.07 \text{ eV}$
- Shaded regions can be taken according to CP-phases for  $m_{1(\text{or } 3)} = 0.07 \text{ eV}$

# Mass squared differences at $\mu = 10^{14}$ GeV

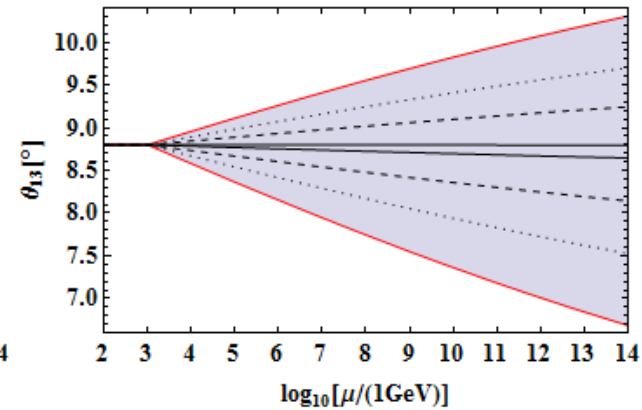
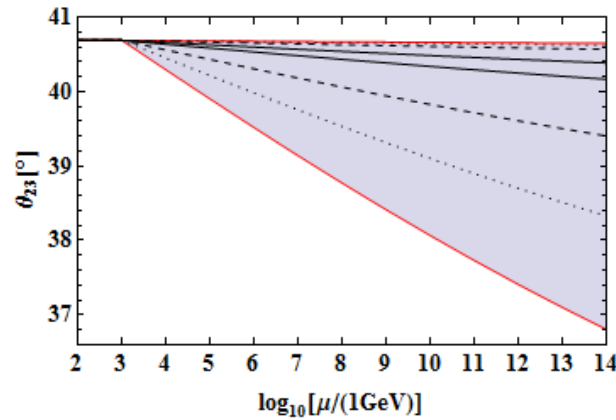
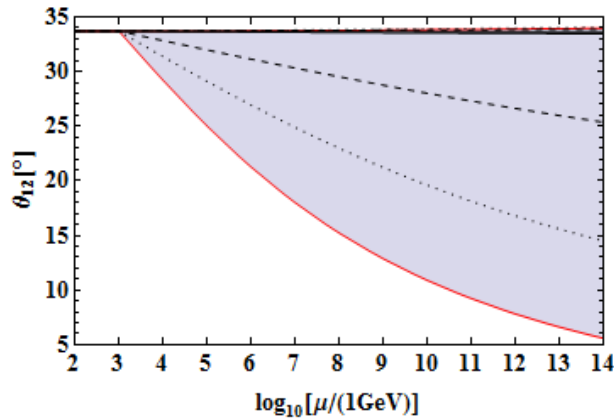


- ○(Red): Including the decoupling effects
- + (Blue): Not including the decoupling effects
  - The clusters correspond to  $m_{1(\text{or } 3)} = 0, 0.01, 0.02, \dots, \text{and } 0.07$  eV from the bottom (top) in the NH (IH)
- The allowed parameters with the decoupling effects are about **3% lower** than those without the decoupling effects

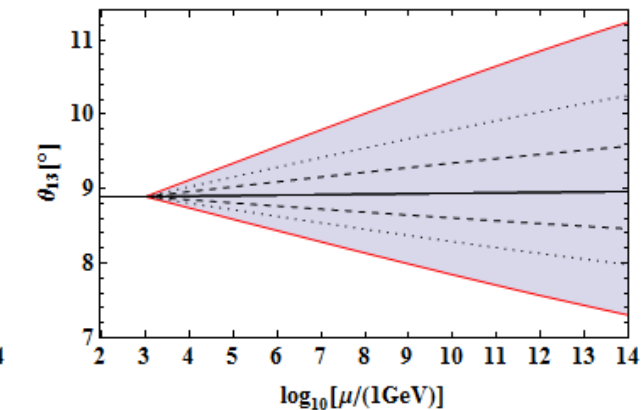
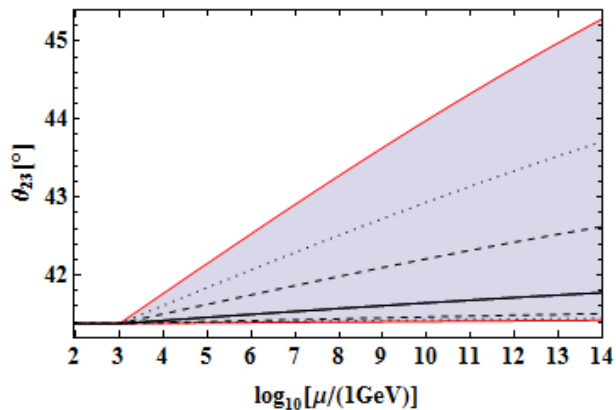
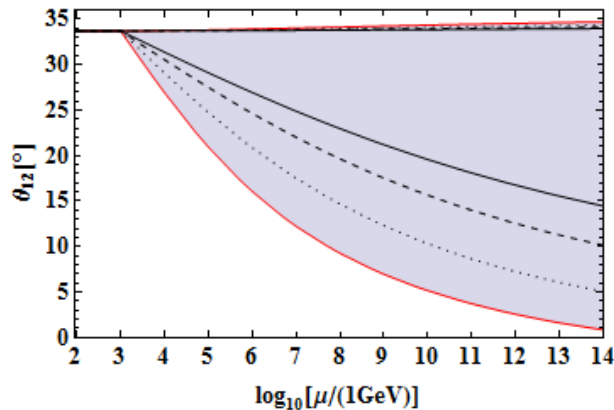


# Runnings of mixing angles

NH (SUSY = 1TeV,  $\tan\beta = 30$ )



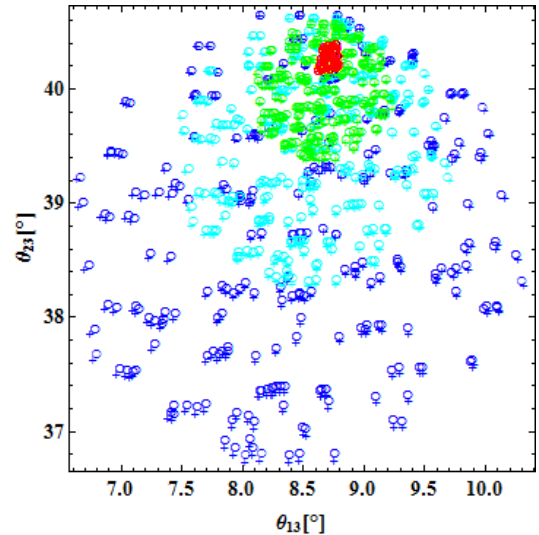
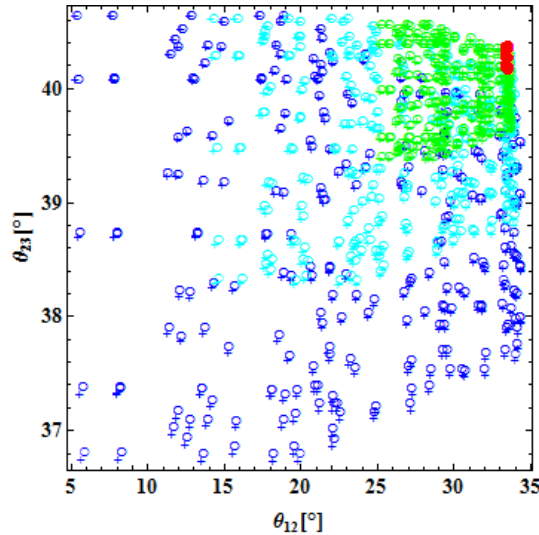
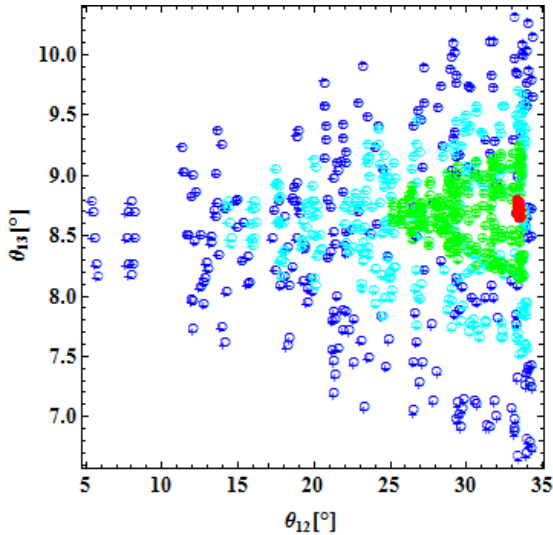
IH (SUSY = 1TeV,  $\tan\beta = 30$ )



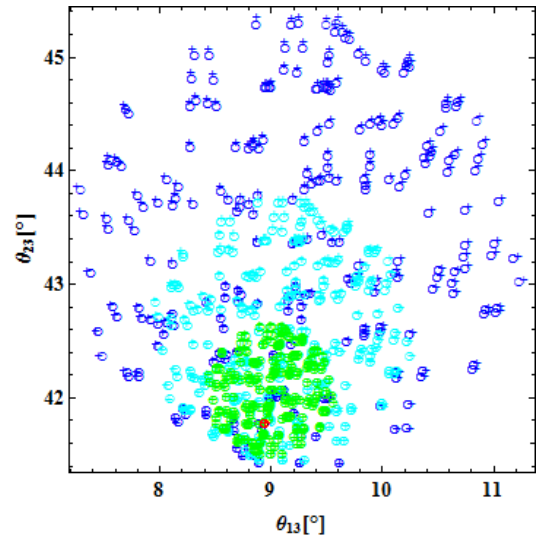
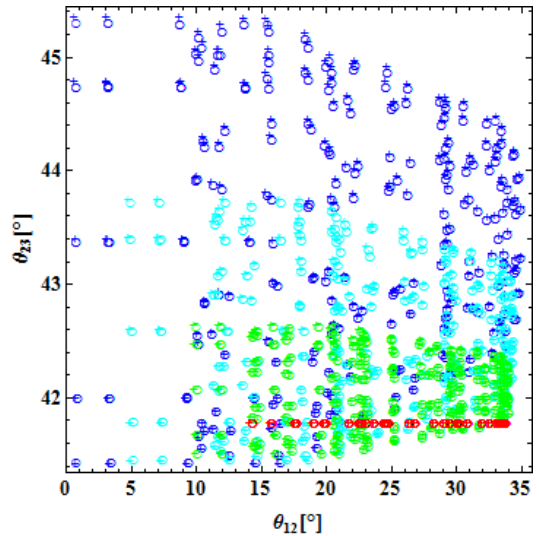
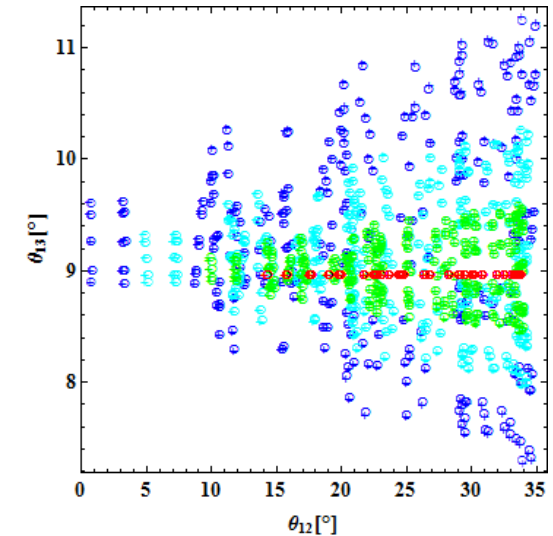
- These figures are the results with the decoupling effects
- Solid, dashed, dotted, and red-solid lines:  $m_{1(\text{or } 3)} = 0, 0.03, 0.05, \text{ and } 0.07 \text{ eV}$
- Shaded regions can be taken according to CP-phases for  $m_{1(\text{or } 3)} = 0.07 \text{ eV}$

# mixing angles at $\mu = 10^{14}$ GeV

NH  
(SUSY = 1TeV,  
 $\tan\beta = 30$ )



IH  
(SUSY = 1TeV,  
 $\tan\beta = 30$ )



- ○ : Including the decoupling effects
- + : Not including the decoupling effects

There are almost no differences between "○" and "+".

# Summary

- We have considered the decoupling effects of top and Higgs
  - Usually these effects are ignored
- The effects of top quark decoupling are negligible for mixing angles but mass eigenvalues
  - When we build models in high energy scale, we should be careful about the difference
- Phenomenological aspects
  - $r \simeq \bar{m} = \sqrt{m_1^2 + m_2^2 + m_3^2}$  is a parameter which give a bound of right-handed neutrino mass in leptogenesis
  - Decay rate of  $0\nu\beta\beta$  decay is proportional to  $(M_\nu)_{ee} = r \times (M_\nu(M_Z))_{ee}$

# Appendix

# EFT in type-I seesaw mechanism

- The analysis only with Weinberg operator is not always possible

– Type-I seesaw ( $M_{N1} < M_{N2} < M_{N3}$ ) M. Lindner, et. al, JHEP 0503(2005)

①  $\mu > M_{N3}$

$$(M_\nu)_{ij} = \sum_{k=1}^3 \frac{(Y_\nu^T)_{ik}(Y_\nu)_{kj}}{(M_N)_k} v^2$$

  $N_3$  decouple

②  $M_{N2} < \mu < M_{N3}$

$$(M_\nu)_{ij} = \kappa_{ij} v^2 + \sum_{k=1}^2 \frac{(Y_\nu^T)_{ik}(Y_\nu)_{kj}}{(M_N)_k} v^2$$

  $N_2$  decouple

③  $M_{N1} < \mu < M_{N2}$

$$(M_\nu)_{ij} = \kappa_{ij} v^2 + \sum_{k=1}^1 \frac{(Y_\nu^T)_{ik}(Y_\nu)_{kj}}{(M_N)_k} v^2$$

④  $\mu < M_{N1}$

$$(M_\nu)_{ij} = \kappa_{ij} v^2$$

  $N_1$  decouple

When  $\mu < M_{N1}$ , we can analyze only with Weinberg operator

# Merit of using $r$ and $\epsilon$

$$M_\nu(\Lambda) \simeq r \begin{pmatrix} (M_\nu(\Lambda_{EW}))_{ee} & (M_\nu(\Lambda_{EW}))_{e\mu} & (M_\nu(\Lambda_{EW}))_{e\tau} (1 + \epsilon) \\ (M_\nu(\Lambda_{EW}))_{e\mu} & (M_\nu(\Lambda_{EW}))_{\mu\mu} & (M_\nu(\Lambda_{EW}))_{\mu\tau} (1 + \epsilon) \\ (M_\nu(\Lambda_{EW}))_{e\tau} (1 + \epsilon) & (M_\nu(\Lambda_{EW}))_{\mu\tau} (1 + \epsilon) & (M_\nu(\Lambda_{EW}))_{\tau\tau} (1 + \epsilon)^2 \end{pmatrix}$$

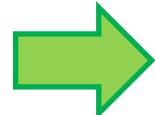
- $r$  and  $\epsilon$  are calculated by

$$r(\Lambda) = \frac{(M_\nu(\Lambda))_{ee}}{(M_\nu(\Lambda_{EW}))_{ee}} \quad \text{and} \quad \epsilon(\Lambda) = \exp \left[ \frac{1}{2} \frac{C_E}{8\pi^2} \int_{t_{EW}}^{t_\Lambda} dt (y_\tau^2 - y_e^2) \right] - 1$$

- We have to solve only **1** RGE for  $M_\nu(\kappa)$
- We can extract mass eigenvalues and mixing angles from  $M_\nu$  at arbitrary energy scale
  - We usually solve **6** RGEs for them (3 mass eigenvalues + 3 mixing angles)
- It is easy to understand the light neutrino's behavior
  - Mass eigenvalues depend on both  $r$  and  $\epsilon$ , but mainly depend on  $r$
  - Mixing angles depend on only  $\epsilon$

# RGEs for gauge couplings

$$16\pi^2 \frac{dg_A}{dt} \equiv 16\pi^2 \beta_{g_A} = b_A g_A^3$$



$$g_A^2(\Lambda) = \frac{g_A^2(\Lambda_{EW})}{1 - \frac{b_A}{16\pi^2} g_A^2(\Lambda_{EW}) \log\left(\frac{\Lambda}{\Lambda_{EW}}\right)^2}$$

- SM

$$\left\{ \begin{array}{l} b_1 = \frac{2}{3} \frac{3}{5} \left[ \left(\frac{1}{6}\right)^2 6N_Q + \left(\frac{2}{3}\right)^2 3N_U + \left(\frac{1}{3}\right)^2 3N_D + \left(\frac{1}{2}\right)^2 2N_L + N_E \right] + \frac{1}{3} \frac{3}{5} \left(\frac{1}{2}\right)^2 2N_H \\ b_2 = -\frac{11}{3} 2 + \frac{2}{3} \frac{1}{2} (3N_Q + N_L) + \frac{1}{3} \frac{1}{2} N_H \\ b_3 = -\frac{11}{3} 3 + \frac{2}{3} \frac{1}{2} (2N_Q + N_U + N_D) \end{array} \right.$$

$$\downarrow N_Q = 3, N_U = 3, N_D = 3, N_L = 3, N_E = 3, N_H = 1$$

$$(b_1, b_2, b_3) = \left( \frac{41}{10}, -\frac{19}{6}, -7 \right)$$

- For the MSSM, we can get  $(b_1, b_2, b_3) = \left( \frac{33}{5}, 1, -3 \right)$  in the same way.

# RGEs in the MSSM

$$\begin{aligned}
 16\pi^2\beta_\kappa &= (Y_E^\dagger Y_E)^T \kappa + \kappa (Y_E^\dagger Y_E) + 2 \operatorname{Tr} \left[ 3Y_U^\dagger Y_U \right] \kappa - \frac{6}{5}g_1^2 \kappa - 6g_2^2 \kappa, \\
 16\pi^2\beta_{Y_U} &= Y_U \left\{ 3Y_U^\dagger Y_U + Y_D^\dagger Y_D + \operatorname{Tr} \left[ 3Y_U^\dagger Y_U \right] - \frac{13}{15}g_1^2 - 3g_2^2 - \frac{16}{3}g_3^2 \right\}, \\
 16\pi^2\beta_{Y_D} &= Y_D \left\{ 3Y_D^\dagger Y_D + Y_U^\dagger Y_U + \operatorname{Tr} \left[ 3Y_D^\dagger Y_D + Y_E^\dagger Y_E \right] - \frac{7}{15}g_1^2 - 3g_2^2 - \frac{16}{3}g_3^2 \right\}, \\
 16\pi^2\beta_{Y_E} &= Y_E \left\{ 3Y_E^\dagger Y_E + \operatorname{Tr} \left[ 3Y_D^\dagger Y_D + Y_E^\dagger Y_E \right] - \frac{9}{5}g_1^2 - 3g_2^2 \right\}.
 \end{aligned}$$

S.Antusch, J.Kersten, M.Lindner, M.Ratz, and M.A.Schmidt (2005)



# How to calculate the RGEs

- In Landau gauge, contributions of electroweak gauge bosons are calculated by the following two diagrams



The solid, dashed, and wavy lines show fermions, Higgs boson, and gauge bosons, respectively.

# Boundary conditions

- To solve the RGEs, we take the boundary conditions for fermions and bosons as below:

$$m_u = 2.3 \text{ MeV}, \quad m_c = 1.28 \text{ GeV},$$

$$m_d = 4.8 \text{ MeV}, \quad m_s = 95 \text{ MeV}, \quad m_b = 4.18 \text{ GeV},$$

$$m_e = 0.511 \text{ MeV}, \quad m_\mu = 106 \text{ MeV}, \quad m_\tau = 1.78 \text{ GeV},$$

$$M_Z = 91.2 \text{ GeV}, \quad m_h = 126 \text{ GeV},$$

$$\alpha_{em}^{-1} = 127.944, \quad \sin^2 \theta_w = 0.23116, \quad \alpha_s \equiv g_3^2/(4\pi) = 0.1184,$$

at  $\mu = M_Z$ , and  $m_t = 160 \text{ GeV}$  at  $\mu = m_t^{pole} = 173 \text{ GeV}$ .

PDG data (2012)

# Matching conditions

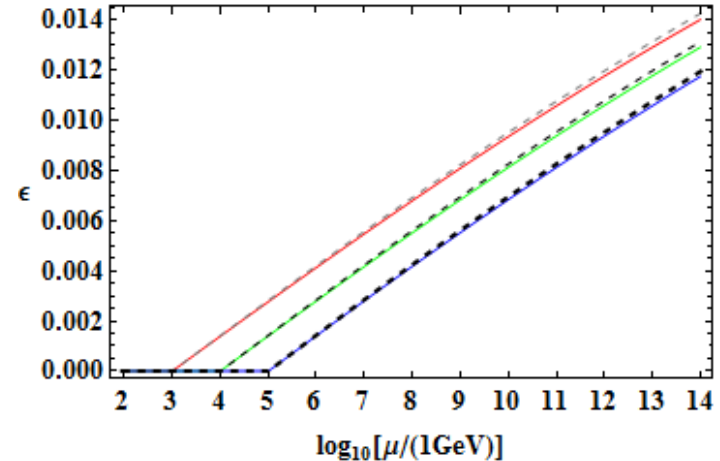
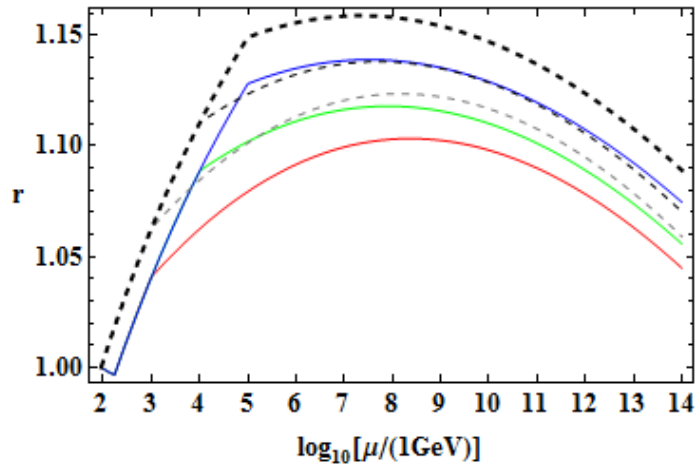
- We use the RGEs at one loop level, and matching conditions at tree level



- The RGEs of  $\kappa$  are continuously connected at the thresholds without the corrections

# SUSY threshold dependence of $r$ and $\epsilon$

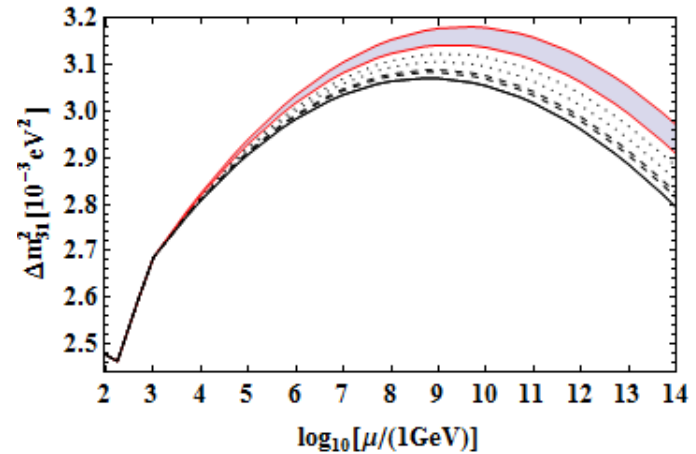
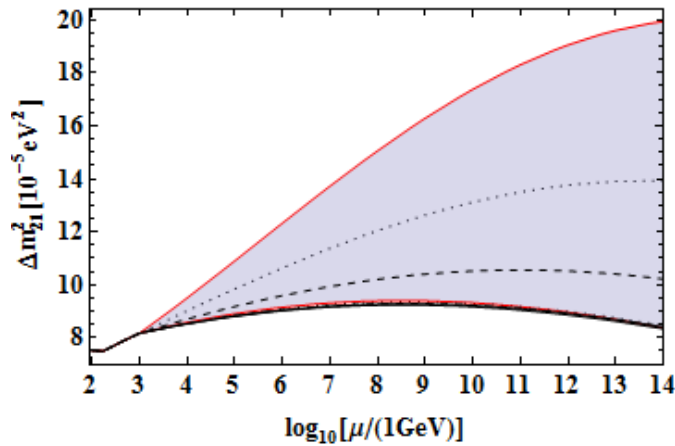
MSSM  
( $\tan\beta = 30$ )



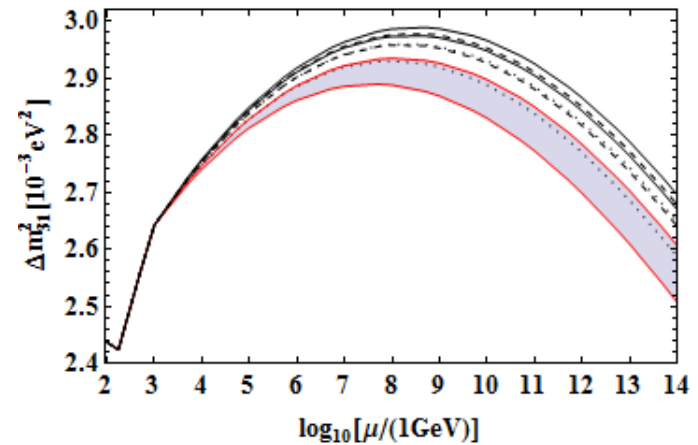
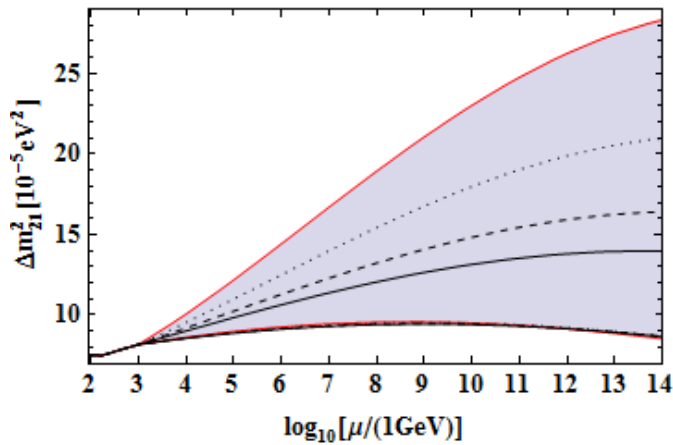
- Solid line: Including the decoupling effects
- Dashed line: Not including the decoupling effects
  - Red, Green, and Blue lines: SUSY = 1, 10, and 100 TeV
- The fundamental behavior is same as before
  - The differences between including the decoupling effects or not are almost independent of SUSY threshold.
- All results for  $r$  and  $\epsilon$  are independent of mass spectrum of the light neutrinos and all CP-phases

# Runnings of mass squared differences

NH  
(SUSY = 1TeV,  
 $\tan\beta = 30$ )



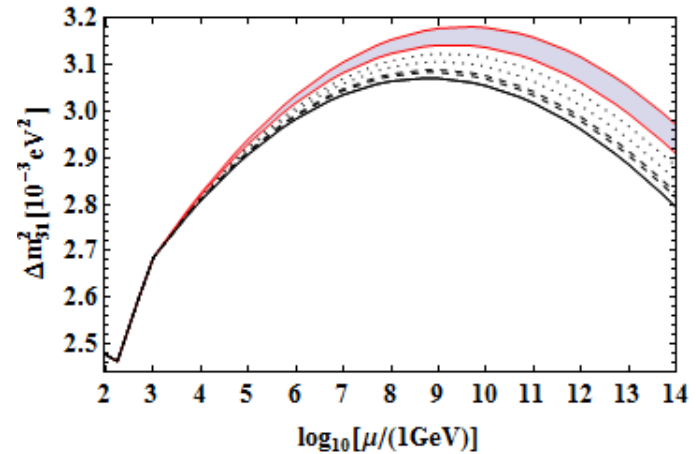
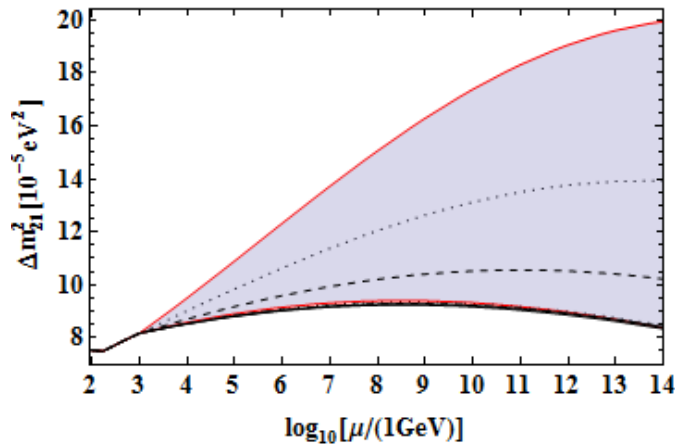
IH  
(SUSY = 1TeV,  
 $\tan\beta = 30$ )



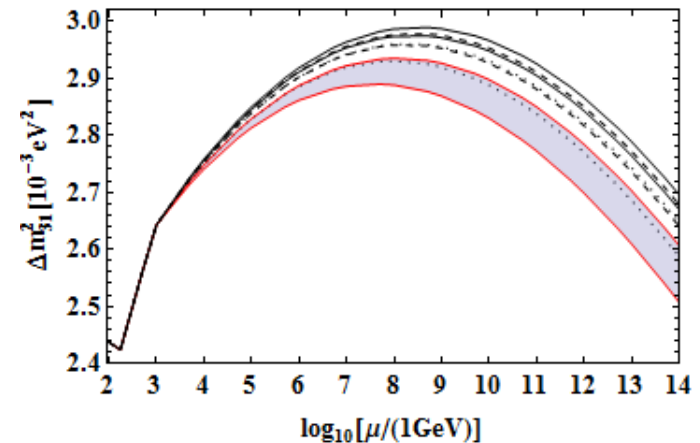
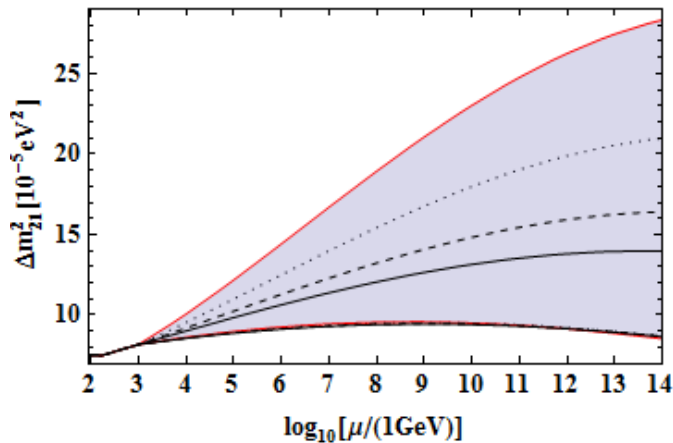
- These figures are results including the decoupling effects
- Solid, dashed, dotted, and red-solid lines:  $m_{1(\text{or } 3)} = 0, 0.03, 0.05, \text{ and } 0.07 \text{ eV}$
- Shaded regions can be taken according to CP-phases for  $m_{1(\text{or } 3)} = 0.07 \text{ eV}$

# Runnings of mass squared differences

NH  
(SUSY = 1TeV,  
 $\tan\beta = 30$ )



IH  
(SUSY = 1TeV,  
 $\tan\beta = 30$ )



- As  $m_{1(\text{or } 3)}$  is large allowed region of  $\Delta m_{21}^2$  is much larger than that of  $\Delta m_{31}^2$ 
  - For  $m_{1(\text{or } 3)} = O(0.01)\text{eV}$ ,  $\Delta m_{21}^2 < m_1^2 < \Delta m_{31}^2$

→  $\Delta m_{21}^2$  is sensitive to the quantum effect of  $m_1$

# Runnings of mass squared differences

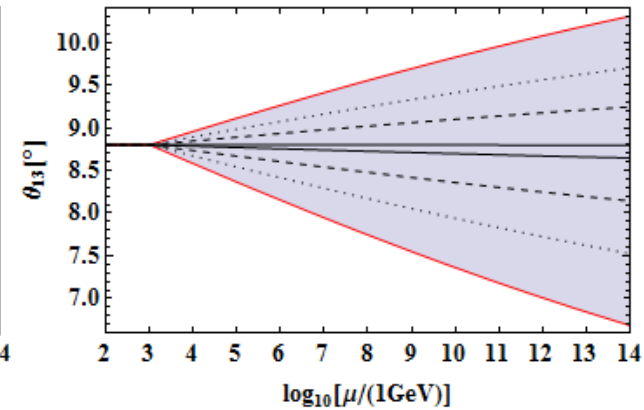
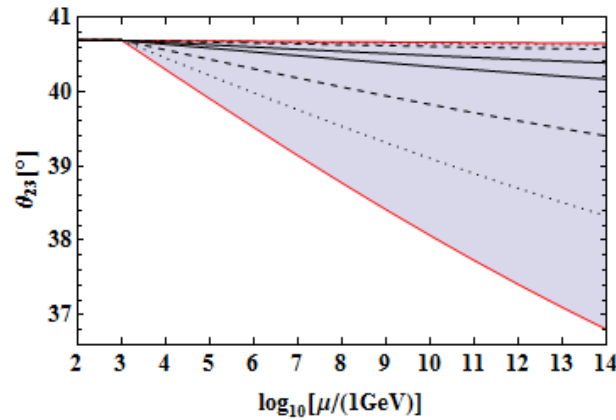
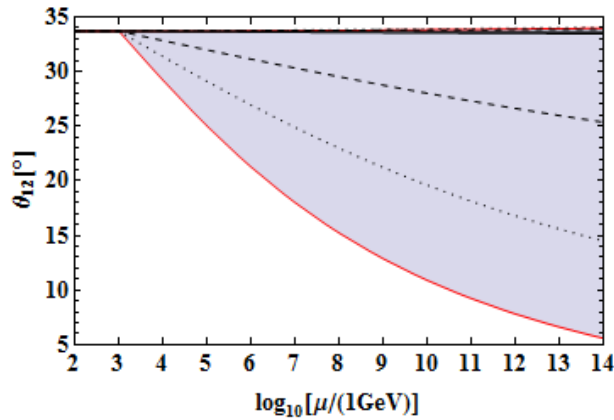
- Combinations of CP-phases which give the upper and lower bounds

| NH          | $\Delta m_{21}^2$  | $\Delta m_{31}^2$  |
|-------------|--|--|
| Upper bound | (0, any, $\pi$ ) / (0, $\pi$ , $\pi$ )                         | (0, any, 0) / (0, 0, 0)  |
| Lower bound | ( $\pi$ , any, 0) / ( $\pi$ , $\pi$ , 0)                       | (0, any, $\pi$ ) / ( $\pi$ , $\pi$ , 0)                        |
| IH          | $\Delta m_{21}^2$  | $\Delta m_{31}^2$  |
| Upper bound | $\delta = 0,  \phi_1 - \phi_2  = 0$ / (0, 0, 0)                | $\delta = \pi,  \phi_1 - \phi_2  = \pi$ / ( $\pi$ , 0, $\pi$ ) |
| Lower bound | $\delta = \pi,  \phi_1 - \phi_2  = \pi$ / ( $\pi$ , 0, $\pi$ ) | $\delta = 0,  \phi_1 - \phi_2  = 0$ / (0, $\pi$ , $\pi$ )      |

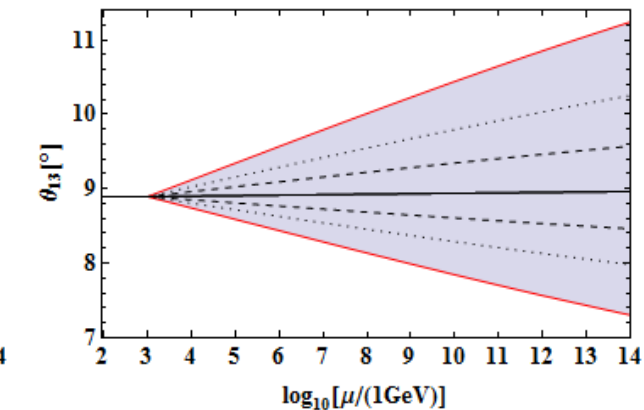
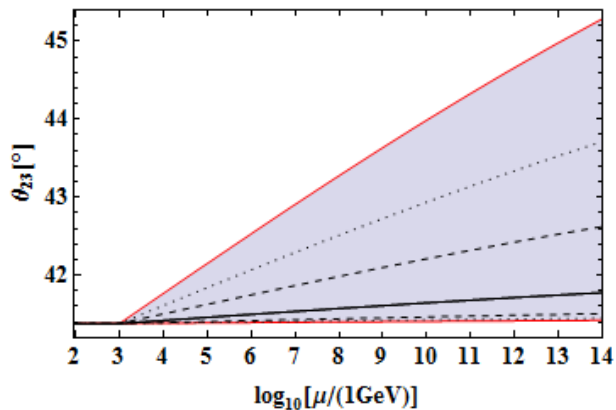
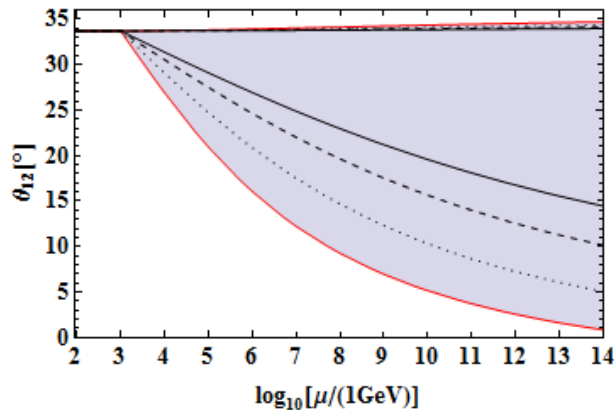
- The values in the table are  $(\delta, \phi_1, \phi_2)$
- The former and latter combinations correspond to  $m_{1(\text{or } 3)} = 0\text{eV}$  and nonzero  $m_{1(\text{or } 3)}$
- For  $m_1 = 0\text{eV}$  in NH, both  $\Delta m_{21}^2$  and  $\Delta m_{31}^2$  are independent of  $\phi_1$
- For  $m_3 = 0\text{eV}$  in IH, they are independent of  $|\phi_1 - \phi_2|$
- The upper and lower parts of the allowed regions (except  $\Delta m_{31}^2$  in IH) are taken by  $\delta = 0$  and  $\pi$ , respectively
- For  $\Delta m_{31}^2$  in IH, they are taken by  $\delta = \pi$  and 0, respectively

# Runnings of mixing angles

NH (SUSY = 1TeV,  $\tan\beta = 30$ )



IH (SUSY = 1TeV,  $\tan\beta = 30$ )



- These figures are the results with the decoupling effects
- Solid, dashed, dotted, and red-solid lines:  $m_{1(\text{or } 3)} = 0, 0.03, 0.05, \text{ and } 0.07 \text{ eV}$
- Shaded regions can be taken according to CP-phases for  $m_{1(\text{or } 3)} = 0.07 \text{ eV}$



# Runnings of mixing angles

- Combinations of CP-phases which give the upper and lower bounds

| NH          | $\theta_{12}$                            | $\theta_{23}$                          | $\theta_{13}$                          |
|-------------|--|--|--|
| Upper bound | depend on $m_1$                          | $(0, \text{any}, \pi) / (0, \pi, \pi)$ | $(\pi, \text{any}, 0) / (\pi, \pi, 0)$ |
| Lower bound | $(\pi, \text{any}, 0) / (\pi, \pi, \pi)$ | $(0, \text{any}, 0) / (0, 0, 0)$       | $(0, \text{any}, 0) / (\pi, 0, \pi)$   |

| IH          | $\theta_{12}$                                       | $\theta_{23}$         | $\theta_{13}$       |
|-------------|---|-----------------------|---------------------|
| Upper bound | depend on $m_3$                                     | - / $(\pi, 0, 0)$     | - / $(\pi, 0, \pi)$ |
| Lower bound | $\delta = \pi,  \phi_1 - \phi_2  = 0 / (\pi, 0, 0)$ | - / $(\pi, \pi, \pi)$ | - / $(\pi, \pi, 0)$ |

| $m_1$ (or $m_3$ )            | 0 eV  | 0.03 eV  | 0.05 eV  | 0.07 eV  |    |
|------------------------------|---|--|--|--|----|
| Upper bound of $\theta_{12}$ | $(0, \text{any}, 0)$  | $(0, \pi, 0)$  | $(\frac{\pi}{2}, \frac{3\pi}{2}, \frac{\pi}{2})$<br>or $(\frac{3\pi}{2}, \frac{\pi}{2}, \frac{3\pi}{2})$ | $(\frac{\pi}{2}, \frac{\pi}{2}, \frac{3\pi}{2})$<br>or $(\frac{3\pi}{2}, \frac{3\pi}{2}, \frac{\pi}{2})$ | NH |
|                              | $\delta = \frac{\pi}{2}$ or $\frac{3\pi}{2}$ ,<br>$ \phi_1 - \phi_2  = \pi$ | $(\frac{\pi}{2}, \frac{\pi}{2}, \frac{3\pi}{2})$<br>or $(\frac{3\pi}{2}, \frac{3\pi}{2}, \frac{\pi}{2})$ | $(\frac{\pi}{2}, 0, \pi)$<br>or $(\frac{3\pi}{2}, 0, \pi)$   | $(\frac{\pi}{2}, 0, \pi)$<br>or $(\frac{3\pi}{2}, 0, \pi)$   | IH |

- For  $m_1 = 0\text{eV}$  in NH, all mixing angles are independent of  $\phi_1$
- For  $m_3 = 0\text{eV}$  in IH,  $\theta_{12}$  is independent of  $|\phi_1 - \phi_2|$ , and  $\theta_{23}$  and  $\theta_{13}$  are almost independent of all CP-phases

|              | $\theta_{12}$<br>$ \phi_1 - \phi_2 $ | $\theta_{23}$<br>$(\phi_1, \phi_2)$ | $\theta_{13}$<br>$( \delta - \phi_1 ,  \delta - \phi_2 )$ |
|--------------|--------------------------------------|-------------------------------------|---|
| Upper region | $\pi$                                | $(\pi, \pi)$                        | $(0, \pi)$  |
|              |                                      | $(0, 0)$                            | $(\pi, 0)$  |
| Lower region | 0                                    | $(0, 0)$                            | $(\pi, 0)$  |
|              |                                      | $(\pi, \pi)$                        | $(0, \pi)$  |